RSC Advances

PAPER

View Article Online
View Journal | View Issue

Cite this: *RSC Adv.*, 2020, **10**, 33178

Self-healing microcapsules encapsulated with carbon nanotubes for improved thermal and electrical properties†

V. Naveen, [a] Abhijit P. Deshpande *[b] and S. Raja[a]

Received 31st July 2020
Accepted 30th August 2020

DOI: 10.1039/d0ra06631a

rsc.li/rsc-advances

Microcapsules are widely used by researchers in self-healing composites. In this study, multi-walled carbon nanotubes (CNT) were incorporated into the core of the microcapsules, along with the self-healing agent. Dicyclopentadiene (DCPD) and urea-formaldehyde (UF) were chosen as the core and shell materials respectively, and DCPD–CNT–UF based dual core microcapsules were synthesized. Two types of microcapsules, namely, DCPD–UF and DCPD–CNT–UF were successfully synthesized by the *in situ* polymerization technique. The novelty of this work is the development of dual core microcapsules with DCPD–CNT–UF combination. Surface morphology characterization and elemental analysis of the microcapsules were carried out using a scanning electron microscope (SEM-EDX). TGA and DSC analysis show that DCPD–CNT–UF microcapsules have better thermal stability than DCPD–UF microcapsules. These novel DCPD–CNT–UF microcapsules were found to be compatible with epoxy base resin for making resin castings. The presence of CNT is found to improve the mechanical, thermal and electrical properties of the resin cast specimens without compromising on self-healing efficiency.

1 Introduction

The usage of polymer composites increases rapidly with time, in various applications, especially in aerospace and wind energy mills. Upon usage, polymer composite structures are subjected to severe environmental conditions like high pressure and temperature. Over the period of time, micro-cracks may be formed on the composite surfaces and propagate through the structure. It is difficult to detect the micro-cracks at the early stages. If we leave the micro-cracks unattended, they develop and propagate deep inside the structure. At some point of time, catastrophic failure of the composite structure may occur. Self-healing composites have the advantages of self-detecting and self-healing the micro-cracks to prevent major structural damage.

Self-healing agents are either encapsulated in the form of microcapsules or filled inside the hollow fibers. When the micro-cracks propagate into the composite structure, the nearby microcapsules break and release the healing agent. The self-healing agent, in the form of liquid monomer, comes out and polymerizes instantaneously in the presence of the surrounding catalyst and the resultant material seals the micro-cracks.[1,2] *In situ* polymerization technique for the synthesis of microcapsules containing self-healing agents is well explained by Brown *et al.*[3] The diameter and shell thickness of the microcapsules mainly depends upon the rate of agitation and chemical composition of the raw materials.[4] Microcapsules with a wide range of dimensions are reported by researchers. Diameter ranging from 10 μm to 1000 μm and shell thickness in the range of 220 nm to 1 μm are reported in the literature.[5–7] Carbene complexes of transition metals are used as the catalyst for the self-healing process in polymer composites. The catalyst works based on ring-opening metathesis-polymerization (ROMP) of the healing agent.[8]

While making SHC, microcapsules create voids and eventually turn into defects in the composite structures. Hence, the self-healing formulation has the adverse effect of reducing the mechanical properties of polymer composites. Therefore, it is important to make up the loss of mechanical properties during the formulations of self-healing composites. The effect of microcapsule diameter, amount of healing agent on mechanical properties, and self-healing efficiency of the composites are discussed in detail by Kanellopoulos *et al.*[9,10] Nano-fillers such as carbon nanotubes (CNT), nano clay, alumina powder are proven to be good additives to improve the mechanical properties of composite materials. Among these nano-fillers, CNT is the primary choice for making polymer composites due to its high strength to weight ratio. The influence of adding CNT, on mechanical and electrical properties of the epoxy nanocomposites is discussed in detail in the literature.[11,12] In addition to improvement in mechanical properties, when 1 wt% of

[a]CSIR, National Aerospace Laboratories, Bangalore, 560017, India. E-mail: naveen.v@nal.res.in; raja@nal.res.in

[b]PECS Laboratory, Department of Chemical Engineering, Indian Institute of Technology-Madras, Chennai, 60036, India. E-mail: abhijit@iitm.ac.in

† Electronic supplementary information (ESI) available. See DOI: 10.1039/d0ra06631a

CNT was incorporated into the epoxy nanocomposites, the electrical conductivity was found to be around 1×10^{-6} S m^{-1}. An optimum mixing ratio of CNT and graphene nano-plates was reported to be 8 : 2, for better electrical and mechanical properties.

Lanzara *et al.*, have done process simulation studies based on molecular dynamics to investigate the possibility of using multi-walled CNT as a nano-reservoir in self-healing materials. They have reported that CNTs play a dual role as a self-healing container, as well as the reinforcement.[13] Guadagno *et al.*,[14] have reported an epoxy resin system filled with multi-walled CNT to improve the curing temperature and electrical conductivity of the system. Ayatollahi *et al.*,[15] have studied the effect of size and concentration of MWCNT on the mechanical and electrical properties of epoxy nanocomposites. It was reported that both electrical conductivity and tensile strength were significantly higher for samples with MWCNT of higher aspect ratio (length/diameter). Caradonna *et al.*,[16] have dispersed MWCNT and graphene platelets of different aspect ratios into the epoxy matrix by calendaring technique and made nano-composites. Results have shown improvement in the electrical and thermal conductivity of the samples. Zhang *et al.*,[17] have reported microcapsules filled with epoxy resin and CNT bundles. These microcapsules were dispersed with cyanate ester matrix and found to be having improved thermal conductivity and fracture toughness.

Polydopamine–CNT–UF based microcapsules were reported by Li *et al.*,[18] for making self-lubricating composites with improved tribological properties. *In situ* polymerization technique is effectively used by researchers for various applications. Zhong *et al.*,[19] have reported a method to anchor atomically dispersed platinum atoms on carbon nano-tubes (Pt–CNT) in an ultra-low temperature solution, to reduce the free energy of Pt atoms in the solution and thus reduce their agglomeration. Xu *et al.*,[20] have fabricated bismuth vanadate ($BiVO_4$) nano-rods by electrospinning and successfully synthesized a core–shell heterojunction by growing molybdenum disulfide nano-sheets (MoS_2) on ($BiVO_4$) nano-rods by solvo-thermal technique. Wang *et al.*,[21] have reported improved catalytic activity for oxygen evolution reaction of ruthenium catalyst by *in situ* method. Clusters of ruthenium and ruthenium oxide nanoparticles were regenerated by pulse laser ablation. This method is claimed to give high-performance and also cost effective.

In this study, the multi-walled CNTs (MWCNTs) were incorporated inside the microcapsules along with the self-healing agent (DCPD). It was aimed that the presence of CNT in the core of the microcapsules, would improve the mechanical, thermal and electrical properties locally at the self-healing sites, and also the overall properties of the composites/resin cast specimens. The influence of DCPD–UF and DCPD–CNT–UF microcapsules on the final properties of resin cast specimens were compared and the results were discussed in detail.

2 Experimental section

Two types of microcapsules, namely dicyclopentadiene–urea formaldehyde (DCPD–UF) and dicyclopentadiene–carbon nanotube–urea formaldehyde (DCPD–CNT–UF) were successfully synthesized by *in situ* polymerization method with an oil-in-water emulsion system. DCPD and MWCNTs are the core materials and poly-urea formaldehyde forms the shell material. Trial experiments were conducted with 0.5, 1.0, 2.0, 2.5, and 5.0 wt% of MWCNT with respect to the DCPD core. It was found that with more than 2.0 wt%, agglomeration of MWCNT started, and the formation of microcapsules was not stable. Therefore, 2.0 wt% of MWCNT with respect to DCPD was used for further experiments. Grubb's 2nd generation catalyst was used for the self-healing process of the microcapsules. Both types of microcapsules were thoroughly investigated for morphology, functional groups, thermal and electrical properties. Resin cast specimens were prepared using these two types of microcapsules and the self-healing process was studied.

2.1 Experimental set up

The experimental set up for synthesizing microcapsules mainly consists of a chemical reaction set up with a fume hood, electrical water bath with a digital temperature controller (Grant Nova-UK), a mechanical stirrer with a three-bladed propeller (IKA instruments-UK) and a digital pH meter. It is to be ensured that propeller blades should not have sharp edges to prevent any damage to the microcapsules while stirring.

2.2 Chemicals and materials

Ethylene maleic anhydride (EMA) copolymer, dicyclopentadiene, and Grubb's 2nd-generation were procured from Sigma-Aldrich, USA. Epoxy resin was purchased from Huntsman India Ltd. Ammonium chloride, urea, resorcinol, sodium hydroxide, hydrochloric acid, 37 wt% formaldehyde solution and 1-octanol were obtained from Merck India Pvt Ltd. Multi-walled CNT with an aspect ratio of 2000 : 1 was purchased from Nanoshel – Mumbai, India.

2.3 Synthesis of microcapsules

The synthesis of both DCPD–UF and DPD–CNT–UF microcapsules are considered as *in situ* polymerization through and oil-in-water emulsion system. DCPD is dispersed as fine droplets under high agitation. During *in situ* polymerization, urea and formaldehyde react in the water phase to form a low molecular weight pre-polymer. As the molecular weight of the pre-polymer increases, it deposits at the DCPD–water interface. The UF ultimately becomes highly cross-linked and forms the microcapsule shell wall.[3]

The reaction mechanism for the polymerization of DCPD is the ring opening metathesis polymerization (ROMP) promoted by ruthenium based Grubb's catalyst at room temperature. It is a complex phenomenon as the second cyclic olefin (cyclopentene) present in DCPD acts as a cross-linking site, producing a polymer to seal the micro-cracks.[37]

In a 500 mL beaker, about 100 mL of deionized water was taken. Multi-walled CNTs of 2.0 wt% with respect to DCPD were dispersed in deionized water and subjected to mechanical stirring at a higher agitator speed (800 rpm) for 60 minutes. Then, other chemicals such as 2.5 wt% of EMA solution, urea,

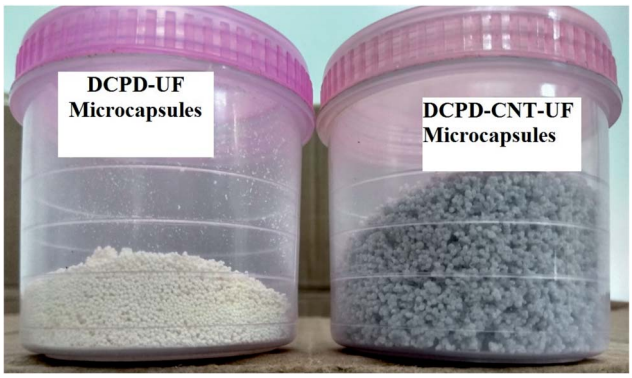

Fig. 1 DCPD–UF and DCPD–CNT–UF microcapsules synthesized in this study.

resorcinol, and ammonium chloride were added and stirred. The agitation speed was reduced to 300 rpm and maintained throughout the reaction process to get microcapsules of the desired size. The pH of the reaction mass was gradually increased from 2.5 to 3.5 by adding NaOH solution. Few drops of 1-octanol were added to prevent the formation of surface bubbles. After 10 minutes, 30 mL of DCPD was added slowly into the beaker, for uniform distribution of DCPD. The reaction mass was allowed to stabilize for 10 minutes, and 6.4 mL of 37 wt% aqueous formaldehyde solution was added. The temperature of the reaction mass was slowly increased to 55 °C at 1 °C min^{-1}. After 4 hours of reaction, agitation was stopped. The reaction mixture was cooled to room temperature, filtered and washed. The microcapsules were air-dried thoroughly for 48 hours to remove the moisture completely. Critical process parameters such as agitation speed, pH, and temperature significantly influence the size and morphology of the microcapsules, and hence to be carefully maintained during the reaction process. Fig. 1 shows the two types of microcapsules synthesized in this work.

2.4 Preparation of resin cast test specimens

Before resin casting, the microcapsules were dried in an electrical oven at 40 °C for 1 h under mild vacuum. Freeze drying of microcapsules was tried once; but found that microcapsules were damaged. Epoxy resin formulation was made using neat resin (LY-556), hardener (HY-951), 5 wt% of microcapsules, and 1 wt% of Grubb's catalyst. Degassing of neat epoxy resin was done by slowly heating the mixture to 50 °C and kept it for 4 hours, under vacuum. Microcapsules and catalyst were dispersed in epoxy resin and carefully mixed using a glass rod, to get a homogeneous mixture. The resin formulation was poured into a glass mould with a 3 mm spacer to form resin castings. Resin cast sheets with neat epoxy, epoxy with DCPD–UF, and DCPD–CNT–UF microcapsules were prepared. As the microcapsules have a higher volume to mass ratio, only 5 wt% of microcapsules were added to make resin casts. A curing cycle of 48 hours at room temperature and 6 hours at 85 °C, was followed for the resin castings. Tensile test specimens as per ASTM standards D-638 (R12.7; 63.5 × 9.5 × 3.2) mm, were prepared from cured resin sheets through a water-jet cutting machine. Various steps involved in making the resin cast specimens are shown in Fig. 2.

2.5 Characterization

Core content analysis was done by the solvent removal method. A known quantity of DCPD–UF microcapsules was weighed on a filter paper and taken in a test tube. About 15 mL of the toluene solvent was added into it. The mixture was crushed well using a glass rod so that all the microcapsules break and DCPD core comes out. Microcapsule and solvent mixture was then washed and filtered several times. Once the core material got washed away with the solvent, the remaining residue (UF shell) was completely dried at 70 °C for 24 hours in a vacuum oven. The dried material was weighed to obtain the final weight of the shell. The ratio of the difference between the microcapsules and shell material to the total microcapsules initially taken, gives the amount of core material originally present in the microcapsules.[22,23] The core content of the microcapsules is calculated as;

$$\%\ \text{core content} = \frac{\text{wt}_{\text{micro-capsule}} - \text{wt}_{\text{shell}}}{\text{wt}_{\text{micro-capsule}}} \times 100$$

The scanning electron microscope, SEM – (LEO 440i with Oxford Energy Dispersive X-ray – UK) was used to analyze the size and morphology of microcapsules. As the microcapsules are non-conductive polymers in nature, they are subjected to gold-sputter coating prior to SEM examination to make the sample conductive and get clear images. Functional groups present in the microcapsules were identified by a Fourier transform infrared spectroscopy with attenuated total reflection (FTIR-ATR, PerkinElmer 1725X) between a wavelength range of 4000 cm^{-1} to 400 cm^{-1}. Pellet samples of both the types of microcapsules were made using potassium bromide powder (KBr) and subjected to FTIR-ATR analysis. The thermal stability of the microcapsules was studied by thermogravimetric analysis (TGA) at 10 °C min^{-1}, from room temperature to 900 °C under the nitrogen atmosphere. Calorimetric measurements were carried out using a differential scanning calorimeter (DSC-205, TA instruments, USA) at 10 °C min^{-1} from room temperature to 400 °C under the nitrogen atmosphere (50 mL min^{-1}). Test results were compared between DCPD–CNT–UF and DCPD–UF type microcapsules. The electrical conductivity of resin cast sample specimens was measured by the 4-probe method at 40 volts input. Thermal conductivity measurement was done for test specimens (10 mm × 10 mm × 3 mm), by hot disc method at 40 °C and 95 °C, and the average test values are reported. The tensile strength of resin cast specimens was tested in a 3 kN, universal testing machine (UTM – Instron) at a displacement rate of 0.2 mm min^{-1}. The average value of four test specimens is reported for tensile strength. The self-healing efficiency of the test specimens was calculated as;

$$\%\ \eta = \frac{(\text{self healed specimen})_{\text{Ts}}}{(\text{virgin specimen})_{\text{Ts}}} \times 100;\ \ \text{Ts} = \text{Tensile strength}$$

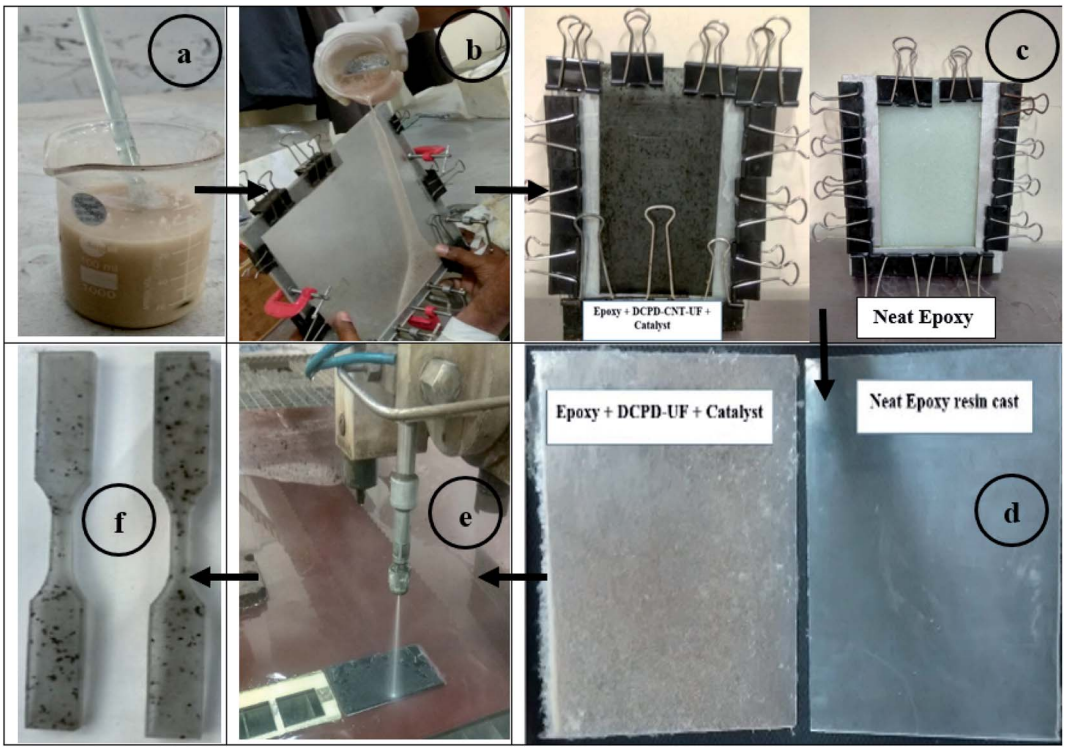

Fig. 2 Various stages of making resin cast specimens: (a) resin formulation, (b) moulding, (c) room temperature curing, (d) post curing (e) waterjet cutting, and (f) sample specimens.

The presence of microcapsules and self-healing are analyzed in an optical microscope (50X) and the fractography of the broken test specimen was done in SEM.

3 Results and discussion

3.1 Core content analysis

The core content of DCPD–UF microcapsules is calculated to be 76%. By a similar experiment, the core content of DCPD–CNT–UF microcapsules is found to be 72%. Normally, microcapsules with thinner shells contain higher core material for the given size of microcapsules. Elemental analysis was done by SEM-EDX for both types of microcapsules (Fig. 3) to cross-check the CNT (carbon content) present in their core region. The results showed that DCPD–CNT–UF microcapsules are having relatively higher carbon content as presented in Table 1.

Table 1 Elemental analysis of microcapsules by SEM-EDX

	DCPD–UF		DCPD–CNT–UF	
Elements	Element%	Atomic%	Element%	Atomic%
C	17.24	25.39	37.35	45.62
O	57.35	63.40	57.08	52.34
Ca	25.41	11.21	5.57	2.04

3.2 Size and surface morphology

DCPD–UF microcapsules are observed to be pale white, while the DCPD–CNT–UF microcapsules are grey in color. Both DCPD–UF and DCPD–CNT–UF microcapsules are spherical in shape with a size ranging from 150 to 550 μm. As shown in

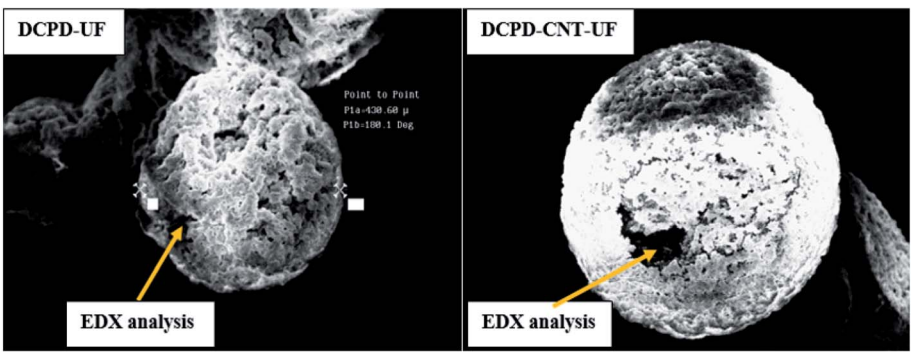

Fig. 3 SEM – EDX analysis of DCPD–UF microcapsules and DCPD–CNT–UF microcapsules.

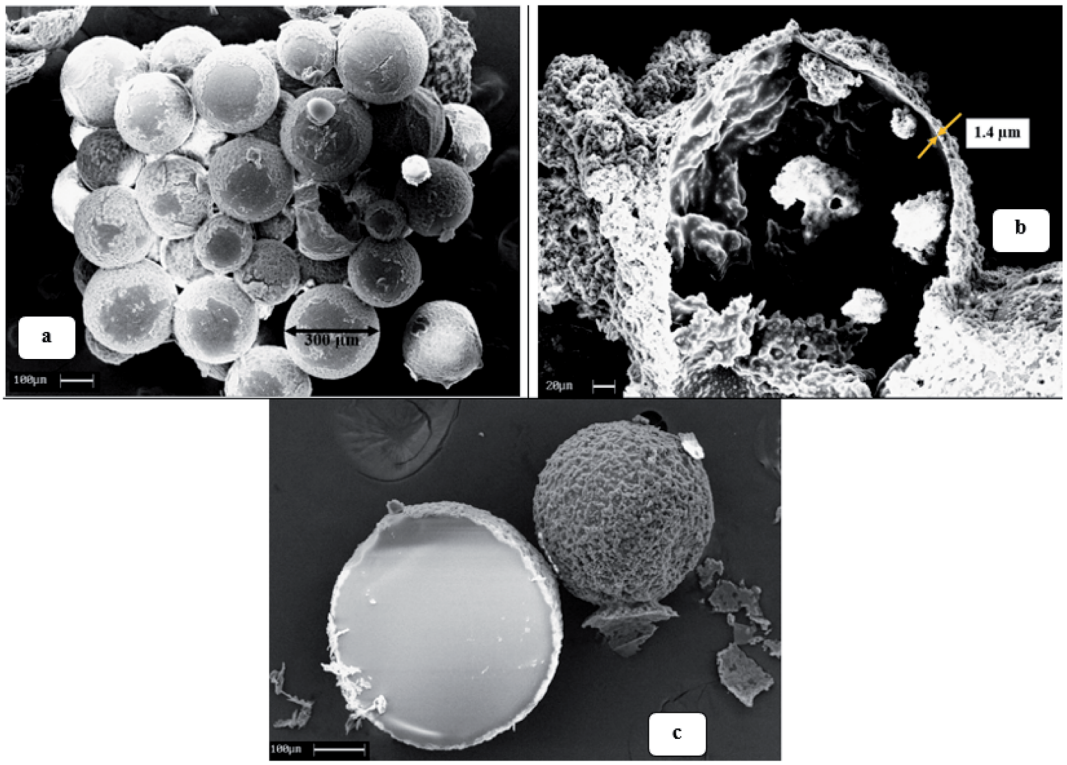

Fig. 4 (a) Size of DCPD–UF microcapsules; (b) cross-sectional view of DCPD–UF microcapsules; (c) surface morphology of DCPD–UF microcapsules.

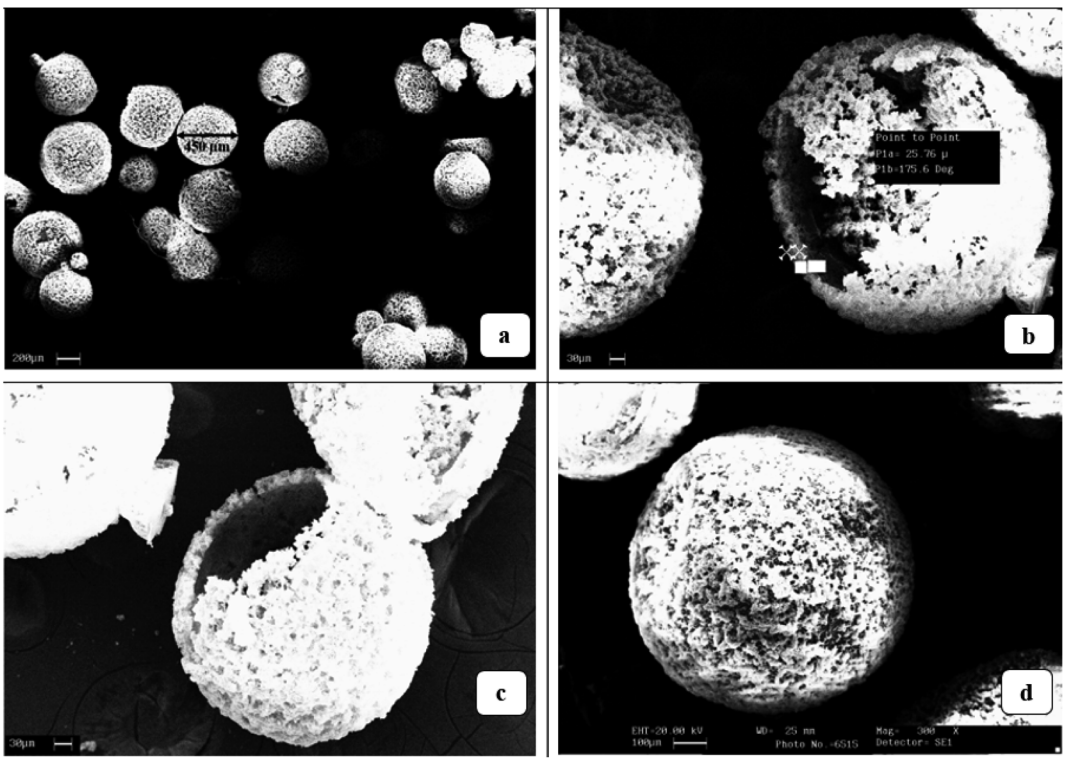

Fig. 5 (a) Size of DCPD–CNT–UF microcapsules; (b) cross-sectional view of DCPD–CNT–UF microcapsules; (c and d) surface morphology of DCPD–CNT–UF microcapsules.

Fig. 4a and b, the average diameter and shell thickness of DCPF–UF microcapsules are 300 μm and 1.4 μm respectively.[24] The surface morphology of DCPD–UF microcapsules is shown in Fig. 4c. A smooth inner surface (DCPD core) and a rough outer surface of the microcapsules were observed.

The agitation speed should not be too high or too less as it affects the mixing pattern and size of the microcapsules. Therefore, an optimum agitation rate of 300 rpm was chosen and maintained throughout the reaction process. It is noticed that the microcapsules have a smooth inner surface because of DCPD core and rough outer surface. As reported in the literature by Brown *et al.*,[3] the rough outer surface of the microcapsules is due to the agglomeration of excess UF during the shell formation. DCPD–UF–CNT microcapsules were measured to be having 450 μm diameter and 25 μm shell thickness respectively. The inner surface of the DCPD–CNT–UF microcapsules is observed to be relatively rougher than the DCPD–UF microcapsules. The addition of MWCNTs into the core along with a healing agent (DCPD) has yielded larger microcpasules with higher shell thickness.

Fig. 5a–d, show the diameter, shell thickness and surface morphology of the DCPD–CNT–UF microcapsules respectively. The process stability and final yield of the DCPD–CNT–UF microcapsules were better compared to DCPD–UF microcapsules. Hence, these dual core (DCPD–CNT–UF) microcapsules with higher shell thickness are expected to improve the mechanical properties locally at the self-healing sites (self-healing efficieny). In addition to it, with higher shell thickness and presence of CNT, these microcapsules will improve the overall properties of the composites such as thermal stability and electrical conductivity. LePing *et al.*,[25] have synthesized epoxy–UF based microcapsules of 100 μm diameter and 4 μm shell thickness by *in situ* polymerization. These microcapsules were made under high agitation rate of 800 rpm.

3.3 Functional group analysis

Functional groups present in the microcapsules are identified by the FTIR-ATR spectrum. The sharp peaks appear at a wavelength of 3060 cm^{-1} and 1465 cm^{-1}, corresponding to the vinyl group (–CH=CH_2) and carbonyl group (C=O) between 1680 and 1630 cm^{-1} confirms the presence of DCPD in both types of microcapsules.[26] The presence of CNT is identified in the DCPD–CNT–UF sample with peaks appearing at 800 cm^{-1} which shows a 44% match with a high carbon content compound, ethyl toluene (C_9H_{12}) from in-built library data of FTIR-ATR. The characteristic peaks at 3418, 3000 to 2920, 1650 and 1556 cm^{-1} in both types of microcapsules represent O–H stretching, C–H stretching, C=O stretching, N–H bending, C–H bending, and C–N stretching, respectively, which confirm the presence of shell material, poly urea-formaldehyde (PUF).[27] The FTIR results on functional groups are presented in Table 2.

3.4 Thermal analysis

3.4.1 Thermogravimetric analysis (TGA). The TGA traces of DCPD–UF and DCPD–CNT–UF microcapsules are shown in Fig. 6. Initially, there was around 30–50% of mass loss is observed at around 100 °C, in both types of microcapsules due to the evaporation of moisture. Significant mass loss is seen at around 170 °C which indicates the evaporation of DCPD. It is further noticed that there is a rapid mass loss between 255 °C to 290 °C, indicating the degradation of UF polymer from the samples.[28] The quantum of mass loss is observed to be higher in this region for DCPD–UF microcapsules. At 320 °C, the wt% of the sample remaining for DCPD–CNT–UF and DCPD–UF microcapsules was around 15 wt% and 2 wt% respectively.

DCPD–UF microcapsules continued to experience rapid mass loss, and the entire mass is lost at around 550 °C. In the case of DCPD–CNT–UF microcapsules, the rate of mass loss gradually decreases beyond 550 °C and 1% mass was present at 895 °C. It is evident that the DCPD–CNT–UF microcapsules are having better thermal stability compared to DCPD–UF microcapsules up to 245 °C. Epoxy–graphene oxide–UF based microcapsules reported by Hicyilmaz *et al.*,[29] have shown thermal stability up to 225 °C. Zheng *et al.*, have synthesized,[30] docosane–graphene oxide–CNT based microcapsules with improved thermal stability up to 260 °C compared to the microcapsules without CNT.

3.4.2 Differential scanning calorimetry. DSC plots of DCPD–UF and DCPD–CNT–UF microcapsules are shown in Fig. 7. There is a qualitative similarity between the two plots. An endothermic peak at around 31 °C is due to the phase transition

Table 2 FTIR data of DCPD–UF and DCPD–CNT–UF microcapsules

Components	Functional groups	Wave numbers (cm^{-1})
DCPD	–CH=CH_2	3060, 1465
	C=C; C=O	1680 to 1630
CNT	C_9H_{12}	800
PUF	O–H	3418
	C–H	3000–2920
	–C=O	1650
	–C–N	1556, 1184
	N–H	1535

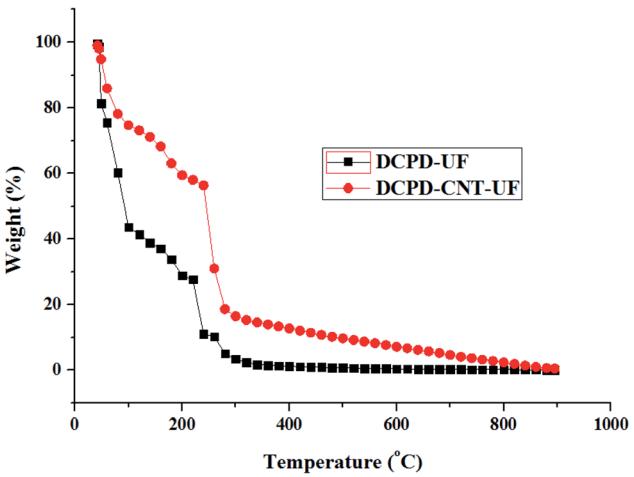

Fig. 6 TGA traces of DCPD–UF and DCPD–UF–CNT microcapsules.

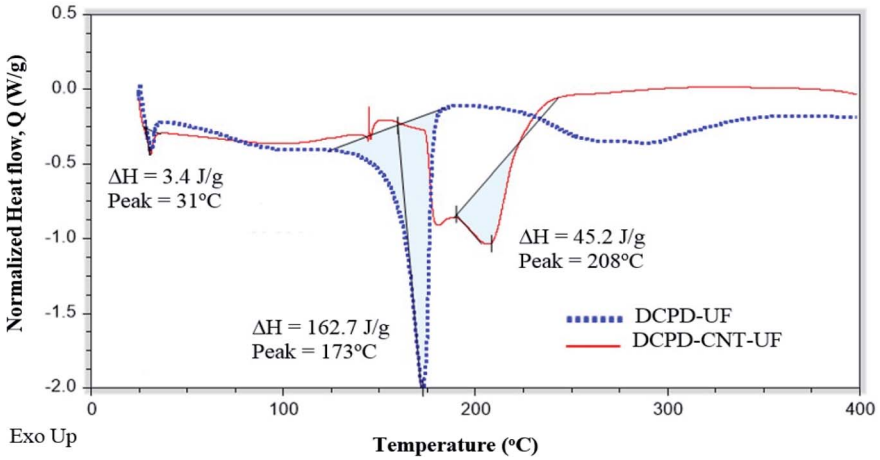

Fig. 7 DSC plots of DCPD–UF and DCPD–CNT–UF microcapsules.

of the DCPD core indicating its melting point. Endothermic peaks between 160 °C and 180 °C are due to the evaporation loss of DCPD indicating its boiling range.[31] A decrease in heat flow values just after 200 °C indicates the degradation of UF shell material. It is noticed that the heat flux curves of both the samples cross-over at 230 °C. Higher heat flow (162.7 J g^{-1}) of DCPD–UF microcapsules indicate that, they are more reactive and unstable. The heat flow value of DCPD–CNT–UF microcapsules are significantly less (45.2 J g^{-1}), which proves that the microcapsules are thermally stable due to the CNT content.

Table 3 Electrical conductivity of epoxy resin cast specimens

Sample name	Electrical resistivity (ohm cm)	Electrical conductivity (S cm^{-1})
Neat epoxy resin cast	14.39×10^{11}	0.695×10^{-12}
Epoxy + 5wt% DCPD–UF microcapsules	4.291×10^{11}	2.33×10^{-12}
Epoxy + 5wt% DCPD–CNT–UF microcapsules	1.915×10^{11}	5.22×10^{-12}

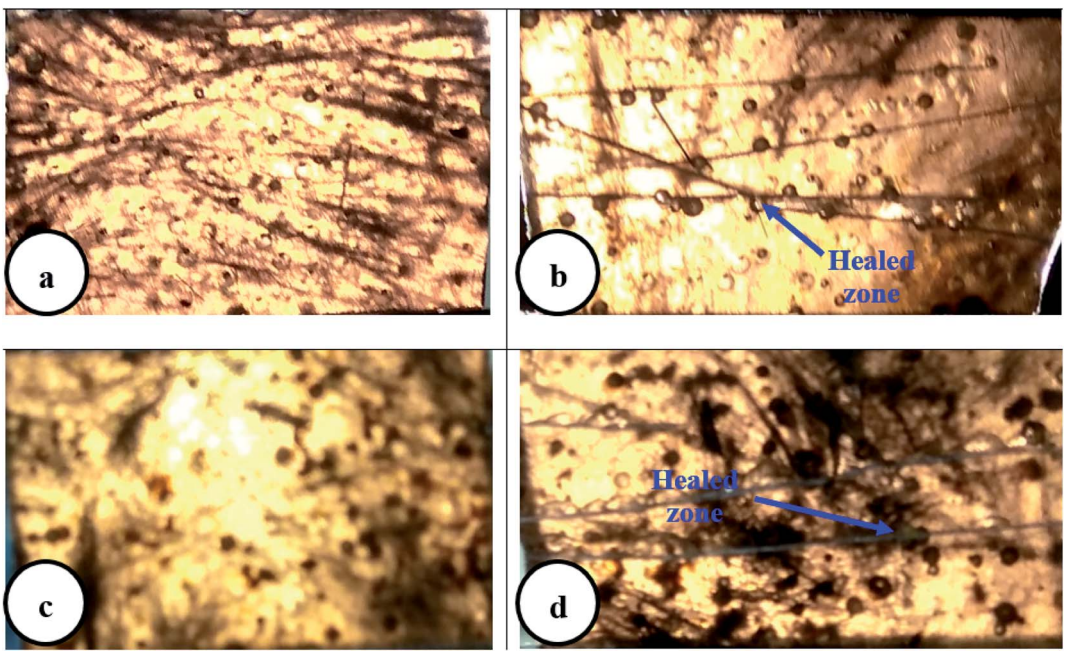

Fig. 8 (a) Virgin composite sample with DCPD–UF microcapsules; (b) self-healed composite sample with DCPD–UF microcapsules; (c) virgin composite sample with DCPD–CNT–UF microcapsules and (d) self-healed composite sample with DCPD–CNT–UF microcapsules.

Table 4 Self-healing efficiency and mechanical property of different epoxy cast specimens

Sample ID	Condition	Tensile strength (MPa)	Healing efficiency η (%)
Neat epoxy	—	40.25	—
Epoxy + 5% DCPD–UF microcapsules	Virgin	30.8	68.8
	After self-healing	21.2	
Epoxy + 5% DCPD–CNT–UF microcapsules	Virgin	32.0	73.4
	After self-healing	23.5	

DCPD–UF–CNT sample exhibits better thermal stability compared to DCPD–UF for the remaining heating range (230 °C to 400 °C) due to the presence of MWCNTs.

3.5 Electrical and thermal conductivity

The average electrical conductivity values of the samples with a measurement error of ±2% are given in Table 3. Resin cast specimens with 5 wt% of DCPD–CNT–UF microcapsules are found to be having slightly higher electrical conductivity compared to resin cast specimens with 5 wt% of DCPD–UF microcapsules. The electrical conductivity of samples with DCPD–CNT–UF microcapsules are found to be significantly higher compared to DCPD–UF microcapsules (1.24 times) and neat epoxy samples (6.51 times). Wang *et al.*,[32] have reported that graphene-hexamethoxymethylmelamine (HMMM) based microcapsules when mixed with the bitumen sample, the electrical resistivity has significantly reduced from 1.25×10^{13} ohm m to 9.0×10^{8} ohm m.

Similarly, the thermal conductivity of epoxy resin cast specimens was measured by the hot disc method. The average value of test specimens with DCPD–CNT–UF microcapsules is found to be 0.145 W m^{-1} K^{-1}, which is roughly 20% higher compared to the test specimens with DCPD–UF microcapsules and neat epoxy samples (~0.12 W m^{-1} K^{-1}). Octodecane–CNT–melamine formaldehyde based microcapsules were developed by Cui *et al.*,[33] and reported that the thermal conductivity of the microcapsules has improved by 25% (0.115 W m^{-1} K^{-1}), with the addition of 1.67 wt% CNT. Zhang *et al.*,[34] have reported that the thermal conductivity of CNT–epoxy polymer composites has improved by 26% with the addition of 0.5 wt% of CNT compared to neat epoxy samples.

3.6 Self-healing efficiency

Epoxy resin cast specimens with DCPD–CNT–UF microcapsules were subjected to a tensile test to find out the self-healing efficiency. Micro-cracks were initiated from the surface of resin cast specimens using a sharp razor blade. The specimens were then allowed to self-heal at room temperature for 24 h. Self-healed specimens were again subjected to a tensile test at a displacement rate of 0.2 mm min^{-1}, and the self-healing efficiency (η) was calculated by a method suggested by Marialuigia and Liberata.[35] The microscope images of the virgin composite specimen without any micro crack, and composite specimens after self-healing are shown in Fig. 8a–d. The presence of microcapsules dispersed in an epoxy matrix, micro-cracks on the surface, and self-healed zones are visible.

The average tensile strength values of the test specimens with ±5% error are presented in Table 4. Test results show that the self-healing efficiency of epoxy specimens with DCPD–CNT–UF microcapsules is marginally higher than the samples with DCPD–UF microcapsules. The presence of CNT inside the microcapsule core is observed to be improving the mechanical property and thus self-healing efficiency of the samples. Blaiszik *et al.*,[6] have reported a healing efficiency of 84% and 69%, based on tensile strength of epoxy composites with DCPDF–UF microcapsules of 1 vol% and 2 vol% respectively.

In this study, polymer cross-linking occurs in two places. Cross-linking of urea-formaldehyde (UF) takes place during the synthesis of microcapsules. Cross-linking of poly-DCPD occurs in the composite during the self-healing process. As the UF shell is thinner, and poly-DCPD is present throughout the self-healed zones of the composite sample, measurement of cross-liking degree for these polymers was not possible. However, literature report states that the cross-linking density of poly-DCPD was higher for Grubb's 1st generation catalyst system compared to the 2nd generation catalyst.[36]

3.7. Fractography

Fractured test specimens after the tensile test, were examined in SEM to check the microstructure of the sample surface. SEM

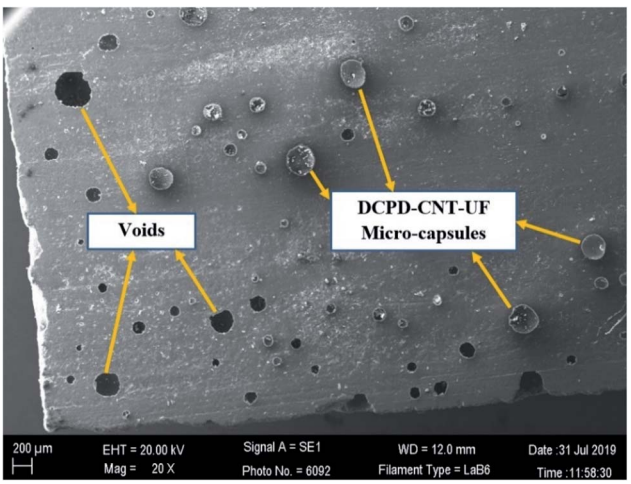

Fig. 9 SEM image of DCPD–CNT–UF resin cast specimen without micro-crack.

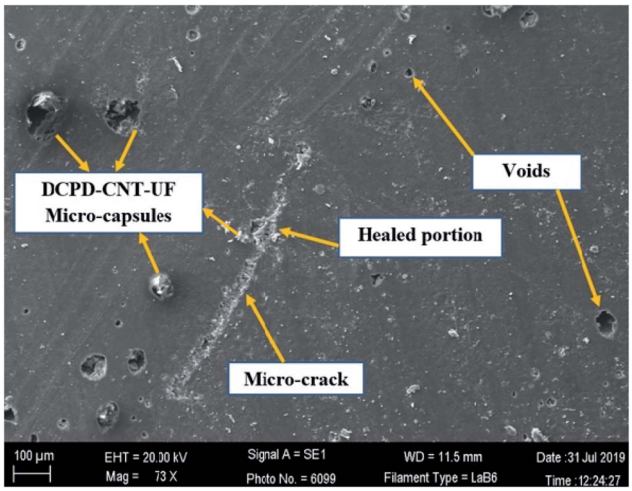

Fig. 10 SEM image of DCPD–CNT–UF resin cast after self-healing.

images in Fig. 9 and 10 suggest that the DCPD–CNT–UF microcapsules are compatible with the epoxy resin matrix. The presence of micro-cracks and healed portions are not clearly seen due to the gold sputter coating on the surface the images are not clear. The presence of microcapsules on the sample surface is visible, but the microcapsules are not distributed uniformly. Also, few voids are seen on the surface of the resin cast samples which indicates that better degassing of epoxy neat resin is required. Complete removal of air bubbles from the resin and uniform distribution of microcapsules inside the resin are still challenging tasks.

A closer view of self-healed zones was seen in an optical microscope images as shown in Fig. 11. The presence of micro-crack, microcapsules present at the SEM sample surface, self-healed, zones at low micro-scale were clearly visible in these high magnified images. The reddish color confirms the presence of Grubb's catalyst.

4 Conclusions

In this work, novel self-healing microcapsules with nano-filled cores were synthesized. Multi-walled nanotubes (CNTs) were successfully incorporated with the dicyclopentadiene (DCPD) core and encapsulated by a urea-formaldehyde (UF) shell, to form dual core microcapsules. Elemental analysis has confirmed a higher carbon content in DCPD–CNT–UF compared to DCPD–UF microcapsules. TGA and DSC studies have shown that DCPD–CNT–UF microcapsules are having better thermal stability than DCPD–UF microcapsules. Tensile strength and self-healing efficiency (73.4%) were also better for resin cast specimens with DCPD–CNT–UF microcapsules, compared to DCPD–UF microcapsules (68.8%). In this study, it is observed that the addition of multi-walled CNT's into the microcapsules has improved the thermal, electrical, and mechanical properties of sample specimens without compromising on self-healing efficiency, thus making it as a multi-functional composite. Moreover, these DCPD–CNT–UF

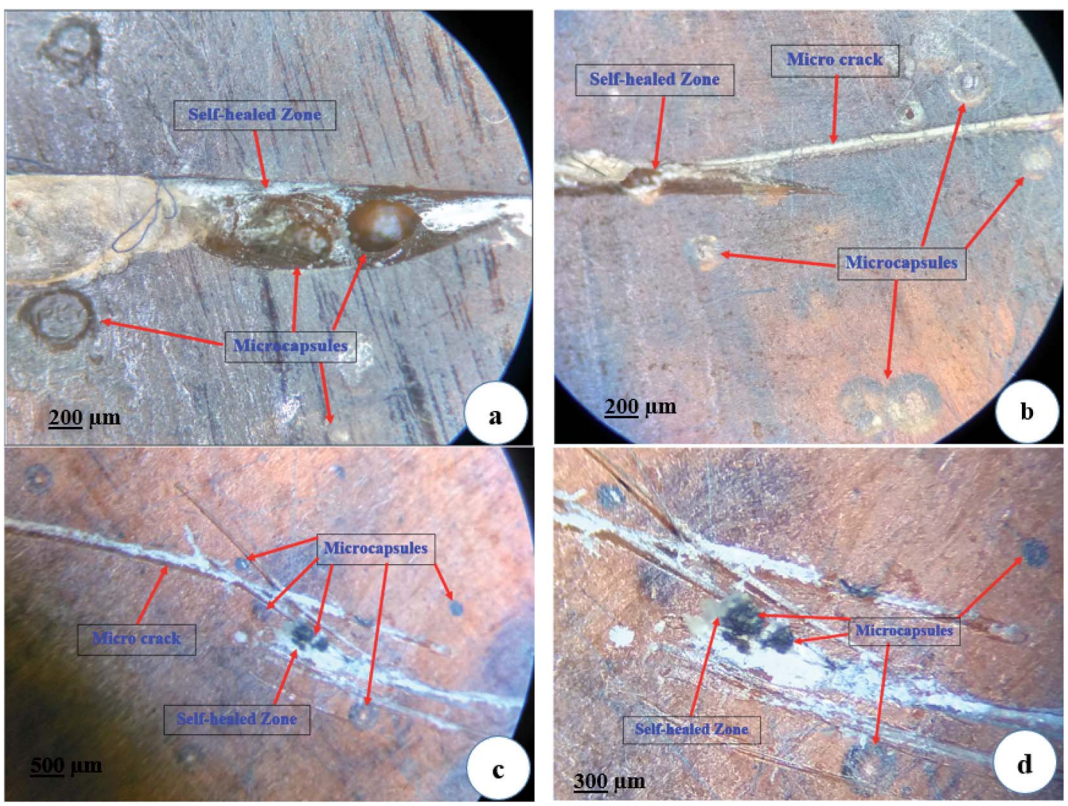

Fig. 11 Optical microscope images of composite specimens showing closer view of self-healed effect.

microcapsules were found to be having better process stability and stronger shell wall compared to the conventional DCPD–UF microcapsules. Resin cast specimens with DCPD–CNT–UF microcapsules were found to be having significant improvement in thermal conductivity (20%) and considerable improvement in electrical conductivity (2.24 times), compared to DCPD–UF microcapsules and neat epoxy samples. Therefore, these novel DCPD–CNT–UF microcapsules can be potential materials to be incorporated in epoxy-based polymer composites for applications such as aerospace, windmills, and automobiles. However, fine-tuning of the quantity of microcapsules to be used in the composite, and uniform distribution of microcapsules into the resin matrix without damaging them are still challenging problems.

Conflicts of interest

There are no conflicts to declare.

Acknowledgements

This research work was funded by Structural Technologies Division (project no: S-0-310), National Aerospace Laboratories (CSIR-NAL), Bangalore-India. We acknowledge Mr S. Vedaprakash (CSIR-NAL, Bangalore) for his technical assistance in making epoxy resin castings and Mr Dasmat Baskey for making tensile test specimen through water-jet cutting. We thank, Mrs Kalavathi, Mr Manikandanath, and Mr Srinivas for SEM-EDX, TGA, and FTIR analysis respectively. We acknowledge Mr Sri Ganesh and Mrs Sheeja Sunil for DSC analysis and tensile tests in UTM respectively. We thank Dr P. K. Panda and Dr Benudhar Sahoo for electrical resistivity measurement.

References

1 S. R. White, N. R. Sottos, P. H. Geubelle, J. S. Moore, M. R. Kessler, S. R. Sriram, E. N. Brown and S. Viswanathan, *Nature*, 2001, **409**, 794.
2 I. L. Hia, V. Vahedi and P. Pasbakhsh, *Polym. Rev.*, 2016, **56**, 225.
3 E. N. Brown, M. R. Kessler, N. R. Sottos and S. R. White, *J. Microencapsulation*, 2003, **20**, 719.
4 R. A. Chowdhury, M. V. Hosur, M. Nuruddin, A. T. Narteh, V. Ashok Kumar, V. Boddu and S. Jeelani, *J. Mater. Res. Technol.*, 2015, **4**, 33.
5 G. Williams, R. Trask and I. Bond, *Composites, Part A*, 2007, **38**(6), 1525.
6 B. J. Blaiszik, N. R. Sottos and S. R. White, *Compos. Sci. Technol.*, 2008, **68**(3–4), 978.
7 H. Ullah, K. Azizi, M. Azizli, Z. B. Man, M. B. C. Ismail and M. I. Khan, *Polym. Rev.*, 2015, **56**(3), 429.
8 M. R. Kessler, N. R. Sottos and S. R. White, *Composites, Part A*, 2003, **34**, 743.
9 J. D. Rule, N. R. Sottos and S. R. White, *Polymer*, 2007, **48**(12), 3520.
10 A. Kanellopoulos, P. Giannaros and A. Al-Tabba, *Constr. Build. Mater.*, 2016, **122**, 577.
11 L. Yue, G. Pircheraghi, S. A. Monemian and I. M. Zloczower, *Carbon*, 2014, **78**, 268.
12 M. R. Zakaria, M. H. Abdul Kudus, M. H. Akil and M. Z. M. Thirmizir, *Composites, Part B*, 2017, **119**, 57.
13 G. Lanzara, Y. Yoon, H. Liu, S. Peng and W. I. Lee, *Nanotechnology*, 2009, **20**, 335704.
14 L. Guadagno, C. Naddeo, V. Vittoria and A. Sorrentino, *J. Nanosci. Nanotechnol.*, 2010, **10**(4), 2686.
15 M. R. Ayatollahi, S. Shadlou, M. M. Shokrieh and M. Chitsazzadeh, *Polym. Test.*, 2011, **30**, 548.
16 A. Caradonna, C. Badini, E. Padovano and M. Pietroluongo, *Materials*, 2019, **12**, 1522.
17 Y. Zhang, L. Yuan, Y. Su, A. Gu, S. Wu and G. Liang, *High Perform. Polym.*, 2016, **29**(4), 396–410.
18 H. Li, Y. Ma, Z. Li, Y. Cui and H. Wang, *Compos. Sci. Technol.*, 2018, **164**, 120.
19 W. Zhong, W. Tu, Z. Wang, Z. Lin, A. Xu, X. Ye, D. Chen and B. Xiao, Ultralow-temperature assisted synthesis of single platinum atoms anchored on carbon nanotubes for efficiently electrocatalytic acidic hydrogen evolution, *J. Energy Chem.*, 2020, **51**, 280.
20 A. Xu, W. Tu, S. Shen, Z. Lin, N. Gao and W. Zhong, $BiVO_4$@MoS_2 core-shell heterojunction with improved photocatalytic activity for discoloration of rhodamine B, *Appl. Surf. Sci.*, 2020, **528**, 146949.
21 Z. Wang, B. Xiao, Z. Lin, S. Shen, A. Xu, Z. Du, Y. Chen and W. Zhong, In-situ surface decoration of RuO_2 nanoparticles by laser ablation for improved oxygen evolution reaction activity in both acid and alkali solutions, *J. Energy Chem.*, 2021, **54**, 510.
22 H. Ullah, K. Azizli, Z. B. Man and M. B. C. Ismail, *Procedia Eng.*, 2016, **148**, 168.
23 R. Wang, H. Hu, W. Liu and Q. Guo, *Polym. Polym. Compos.*, 2011, **19**(4–5), 279.
24 V. Naveen, S. Raja and A. P. Deshpande, *Int. J. Plast. Technol.*, 2019, **23**(2), 157.
25 L. LePing, Z. Wei, X. Yi, W. H. Mei, Z. Yang and L. W. Jun, Preparation and characterization of microcapsule containing epoxy resin and its self-healing performance of anticorrosion covering material, *Chin. Sci. Bull.*, 2011, **56**(4), 439.
26 L. Guadagno and M. Raimondo, *Infrared Spectroscopy – Materials Science Engineering and Technology*, 2012, p. 286, DOI: 10.5772/36029.
27 K. Thanawala, N. Mutneja, A. S. Khanna and R. K. S. Raman, *Materials*, 2014, **7**, 7324.
28 H. H. Noh and J. K. Lee, *eXPRESS Polym. Lett.*, 2013, **7**(1), 88.
29 A. S. Hicyilmaz and A. C. Bedeloglu, In Situ Graphene Oxide Reinforced Poly (Urea - Formaldehyde) Microencapsulation of Epoxy, *Mater. Sci. Res. India*, 2019, **16**(1), 7.
30 Z. Zheng, J. Jin, G. K. Xu, J. Zou, U. Wais, A. Beckett, T. Heil, S. Higgins, L. Guan, Y. Wang and D. Shchukin, *ACS Nano*, 2016, **10**, 4695.
31 S. Then, G. S. Neon and N. H. Abu Kasim, *Sains Malays.*, 2011, **40**(7), 795.
32 X. Wang, Y. Guo, J. Su, X. Zhang, Y. Wang and Y. Tan, *Nanomaterials*, 2018, **8**, 419.

33 W. Cui, Y. Xia, H. Zhang, F. Xu, Y. Zou, C. Xiang, H. Chu, S. Qiu and L. Sun, *Mater. Sci. Eng.*, 2017, **182**, 012015.
34 Y. Zhang, H. Li, P. Liu and Z. Peng, *IEEE International Conference on High Voltage Engineering and Application*, 2016.
35 R. Marialuigia and G. Liberata, *Polym. Compos.*, 2013, **34**, 1525.
36 G. Yang and J. K. Lee, Curing Kinetics and Mechanical Properties of *endo*-Dicyclopentadiene Synthesized Using Different Grubbs' Catalysts, *Ind. Eng. Chem. Res.*, 2014, **53**(8), 3001.
37 T. C. Mauldin and M. R. Kessler, Self-healing polymers and composites, *Int. Mater. Rev.*, 2010, **55**(6), 317.

